
# The glass transition temperature of isolated native, residual, and technical lignin

Wood Physics/Mechanical Properties

Åke Henrik-Klemens, Fabio Caputo, Roujin Ghaffari, Gunnar Westman, Ulrica Edlund, Lisbeth Olsson and Anette Larsson*

# The glass transition temperature of isolated native, residual, and technical lignin

https://doi.org/10.1515/hf-2023-0111
Received November 2, 2023; accepted February 6, 2024;
published online March 5, 2024

**Abstract:** The glass transition temperatures ($T_g$) of native, residual, and technical lignins are important to lignocellulose pulping, pulp processing and side stream utilization; however, how the structural changes from native to residual and technical lignin influences $T_g$ has proven difficult to elucidate. Since the $T_g$ of macromolecules is greatly influenced by the molecular weight, low-molecular-weight fractions, such as milled wood lignin (MWL), are poor representatives of lignin in the cell wall. To circumvent this problem, lignins of both high yield and purity were isolated from Norway spruce and softwood kraft pulp using the enzymatic mild acidolysis lignin (EMAL) protocol. Technical softwood kraft lignin was also fractionated into groups of different molecular weights, to acquire lignin that spanned over a wide molecular-weight range. A powder sample holder for dynamic mechanical analysis (DMA), was used to determine the $T_g$ of lignins, for which calorimetric methods were not sensitive enough. The $T_g$s of EMAL were found to be closer to their *in situ* counterparts than MWL.

**Keywords:** dynamic mechanical analysis; lignocellulose; kraft pulping: thermoplastic properties

***Corresponding author: Anette Larsson**, Applied Chemistry, Chemistry and Chemical Engineering, Chalmers University of Technology, Kemigården 4, SE-412 96 Gothenburg, Sweden; FibRe – Centre for Lignocellulose-Based Thermoplastics, Department of Chemistry and Chemical Engineering, Chalmers University of Technology, SE-412 96 Gothenburg, Sweden; and Wallenberg Wood Science Center, Chalmers University of Technology, Gothenburg, Sweden, E-mail: anette.larsson@chalmers.se
**Åke Henrik-Klemens**, Applied Chemistry, Chemistry and Chemical Engineering, Chalmers University of Technology, Kemigården 4, SE-412 96 Gothenburg, Sweden; and FibRe – Centre for Lignocellulose-Based Thermoplastics, Department of Chemistry and Chemical Engineering, Chalmers University of Technology, SE-412 96 Gothenburg, Sweden
**Fabio Caputo**, Division of Industrial Biotechnology, Department of Life Sciences, Chalmers University of Technology, Kemigården 4, SE-412 96 Gothenburg, Sweden
**Roujin Ghaffari**, Applied Chemistry, Chemistry and Chemical Engineering, Chalmers University of Technology, Kemigården 4, SE-412 96 Gothenburg, Sweden; and Wallenberg Wood Science Center, Chalmers University of Technology, Gothenburg, Sweden
**Gunnar Westman**, FibRe – Centre for Lignocellulose-Based Thermoplastics, Department of Chemistry and Chemical Engineering, Chalmers University of Technology, SE-412 96 Gothenburg, Sweden; Wallenberg Wood Science Center, Chalmers University of Technology, Gothenburg, Sweden; and Organic Chemistry, Chemistry and Chemical Engineering, Chalmers University of Technology, Kemigården 4, SE-412 96 Gothenburg, Sweden
**Ulrica Edlund**, Fibre and Polymer Technology, KTH Royal Institute of Technology, Teknikringen 56, SE-100 44 Stockholm, Sweden; and FibRe – Centre for Lignocellulose-based Thermoplastics, Department of Fibre and Polymer Technology, KTH Royal Institute of Technology, SE-100 44 Stockholm, Sweden
**Lisbeth Olsson**, Division of Industrial Biotechnology, Department of Life Sciences, Chalmers University of Technology, Kemigården 4, SE-412 96 Gothenburg, Sweden; and Wallenberg Wood Science Center, Chalmers University of Technology, Gothenburg, Sweden

## 1 Introduction

Developing materials derived from biomasses is crucial to reduce reliance on fossil resources. Among the biomasses used for industrial material production, those sourced from plants containing substantial amounts of lignin, such as woods and grasses, are particularly interesting due to their large global production. The lignins in these plants play an important role in both their material properties and processing (Back and Salmén 1982); hence, a thorough understanding of the properties of lignin is essential for enabling a shift to sustainable material production. The thermomechanical properties of lignin are especially important, as they play a large role in many aspects of lignocellulosic processing, both conventional and novel.

Industrially, lignins can be divided into three categories: native lignin in untreated biomass, residual lignin in pulped biomass, and technical lignin, which has been isolated from biomass during pulping. As pulping alters the lignin structure, these different types of lignin vary in properties. Likewise, due to chemical and molecular differences, lignins from different botanical origins also vary in properties. To successfully develop new materials from lignin-containing

biomasses and side streams, and to develop and optimize pulping processes, the structure–property relations for these lignins have to be established.

One of the most fundamental thermophysical properties of amorphous polymers such as lignin is its glass transition temperature ($T_g$) – the temperature where the polymer transitions from a glassy solid state to a material where segmental motions of polymer chains facilitate plastic deformation. Lignins generally have a high $T_g$ due to their stiff aromatic backbone and strong secondary interactions (Hatakeyama and Hatakeyama 2010). However, many factors affect the $T_g$ of polymers, including molecular weight and polymer architecture. During kraft pulping, both depolymerization reactions, via the cleavage of the abundant and relatively flexible β-O-4 bonds, and condensation reactions occur. These processes lead to branching and the accumulation of shorter and stiffer linkages, such as 5-5′ and 4-O-5 (Crestini et al. 2017). It is thus obvious that the transition from native to residual and technical lignin drastically changes the thermomechanical properties of lignin. However, the differences in $T_g$ caused by chemical and molecular changes during pulping have not yet been disentangled.

The study of native and residual lignin thermoplasticity is complex: it must be studied either within the cell wall or as an extract. In the cell wall, lignin is held within a complex matrix, and even with sensitive mechanical techniques, it is difficult to differentiate the properties of the different components (Ashaduzzaman et al. 2020). If lignin is extracted, the thermomechanical properties can be studied without influence from other components, and the structure and size of the polymers can be more easily determined, but it is challenging to achieve quantitative non-degrading isolation of lignin.

The $T_g$ of isolated native lignin is typically found to range between 120 and 180 °C (Back and Salmén 1982; Kelley et al. 1987; Pan and Sano 2000), whereas dry wood and pulp softens at temperatures over 200 °C (Salmén and Back 1978; Startsev et al. 2017). The softening of dry wood and pulp has been shown to involve the $T_g$ of lignin (Salmén 1982). The discrepancy in $T_g$ between isolated and *in situ* lignin is likely due to the low yields of many isolation techniques. This is reflected in an early study on the glass transition of lignin by Goring (1963), where successive extractions of lignin from spruce with dioxane isolated successively higher-molecular-weight fractions with increasing $T_g$ (127–172 °C).

In the wake of these earlier studies, new isolation procedures for native and residual lignin have been developed, which extract lignin at a high yield and with little apparent degradation (depolymerization and coupling reactions) (Du et al. 2013; Giummarella et al. 2016, 2019; Wu and Argyropoulos 2003). The enzymatic mild acidolysis lignin (EMAL) protocol developed by Wu and Argyropoulos (2003) is of interest as it isolates with high yield without fractionation, but the thermomechanical properties of EMAL, which would better represent the native material, still need to be determined.

The thermomechanical properties of residual lignins from pulp are also understudied, even though they play a crucial role in the further processing of pulp (Vishtal and Retulainen 2014). Several dynamic mechanical analysis (DMA) investigations have been conducted on water or ethylene glycol-saturated wood samples before and after pulping (Havimo 2009; Heitner and Atack 1984; Vikström and Nelson 1980), which enables differentiation of the $T_g$ of lignin and carbohydrates. These reports typically see a downward shift in $T_g$ after pulping; however, the univocal assignment of transitions in multicomponent systems with DMA is challenging, and plasticizers might plasticize different types of lignins (native or residual) to different degrees, which makes glass transition comparisons uncertain.

Technical lignins, being readily available and the focus of a lot of material development, have been the subject of extensive research. Their $T_g$ values typically fall within the 90–170 °C range, with kraft and soda lignins at the higher end and organosolv lignins at the lower end (Wang et al. 2016). The low $T_g$ of technical lignins can be ascribed to the low molecular weights of these lignins. Organosolv lignins are typically less condensed than kraft lignin (Crestini et al. 2017; El Hage et al. 2010; Karlsson et al. 2023), so it could be expected that these lignins would have a lower $T_g$, but they are also of a lower molecular weight, which prevents a straightforward correlation.

High-yield and high-molecular-weight lignins often lack information on their $T_g$ in the literature. One of the reasons for this could be the difficulty in determining them calorimetrically. Lignin is compositionally heterogeneous and at high molecular weights, the change in heat capacity ($\Delta C_p$) over the glass transition is often not detectable with differential scanning calorimetry (DSC) (Clauss et al. 2015; Fox and McDonald 2010; Souto and Calado 2022).

An alternative technique to calorimetric determinations of the $T_g$ is the above-mentioned DMA. In DMA the mechanical stiffness and energy dissipated in the material under either oscillating stress or strain is measured. These properties change much more drastically over the glass transition than $C_p$, which makes DMA more sensitive; however, the mechanical properties of lignin are difficult to study, as most lignins cannot be cast into continuous shapes, or only very brittle ones. There are examples in the literature of DMA measurements of lignin powders or pressed pellets, typically in a parallel plate setup (Karaaslan et al. 2021; Li and McDonald 2014; Sevastyanova et al. 2014;

Shrestha et al. 2017; Sun et al. 2016). From these measurements, the $T_g$ can be easily determined, and a detailed understanding of the transition is gained. So far, only technical lignins have been subjected to these kinds of DMA measurements, perhaps due to the large sample sizes needed (~500 mg).

This study aims to follow how the kraft pulping process changes the thermomechanical properties of lignin and discern the role of molecular weight and chemical structure on the $T_g$. A powder sample holder for DMA has been adopted to study the thermomechanical properties of lignin isolated in high yield from Norway spruce, and softwood kraft pulp. The powder sample holder allows for the study of small amounts of non-self-supporting amorphous polymers (25–100 mg) (Mahlin et al. 2009), simplifying the study of lignins isolated from biomass. Softwood kraft lignin was also fractionated into groups of different molecular weights, to acquire lignin that spanned a wide molecular-weight range, which could be modeled with the Flory–Fox equation (Fox and Flory 1950). Wheat straw lignin is included as it is a potential source of renewable material, and even though wheat straw lignin has been thoroughly characterized (Zhang et al. 2022), it has never been subjected to thermomechanical characterization at higher yields.

# 2 Materials and methods

## 2.1 Materials

Wood chips were cut from the outer centimeters (sapwood) of Norway spruce (*Picea abies*) timber with a diameter of approximately 15 cm that had been dried for 6 months in-house. Wheat straw (*Triticum aestivum*) was kindly supplied by Lantmännen ekonomisk förening (Stockholm, Sweden), sourced from farms in Sweden. Softwood kraft lignin from the LignoBoost® process was provided from a Swedish pulp mill. The pulp used in the study was an unbleached, never-dried softwood kraft pulp with a lignin content of 13 wt% kindly supplied by Stora Enso AB (Karlstad, Sweden). The softwood kraft lignin and softwood kraft pulp were derived from Norway spruce and pine (*Pinus sylvestris*) of unknown proportions. The cellulase enzyme blend Ctec2® was kindly provided by Novozymes A/S (Bagsværd, Denmark).

## 2.2 Lignin isolation

Lignin from Norway spruce, wheat straw and unbleached softwood kraft pulp were isolated according to the EMAL protocol (Figure 1) (Guerra et al. 2006a,b; Jääskeläinen et al. 2003). Milled wood lignin (MWL) was also isolated from the Norway spruce meal (Björkman 1956). The isolations were conducted according to the references, with some adjustments given below.

Wheat straw leaves and husks were separated by hand, and the soil was washed out with water. Wheat straw and Norway spruce were milled in a knife mill to mesh 40. Extractives were then removed by Soxhlet extraction for 18 cycles in acetone (Fischer scientific, ≥99.8 %), after which the materials were ball milled in a planetary ball mill (Retsch PM 400). Wheat straw was milled for 6 h, and Norway spruce for 18 h. The milling was done in intervals to avoid heating: 30 min milling, and 30 min cooling. The milling was done in air and with no additives.

When received from the mill, the unbleached softwood kraft pulp was slightly alkaline (pH ~ 8) and was subsequently washed repeatedly with tap water until pH neutralized.

The enzymatic hydrolysis was performed in 2 L glass bottles, and the loaded substrate (5 % wt/wt of dry mass (DM)) was suspended in 0.15 M acetate buffer pH 5. The enzymes were loaded based on their activity. Using the filter paper unit (FPU) assay (Ghose 1987) with some adjustments (Novy et al. 2021), the cellulolytic activity in Ctec2® was determined to be 148 FPU/mL. Ctec2 was added at 10 FPU/g DM and after 24 h it was added again using the same loading. The reactions were carried out at 50 °C for 48 h in an incubator with an orbital rotation (INNOVA2100™; New Brunswick Scientific, UK) at 140 rpm. To terminate the reaction, the mixture was boiled for 10 min.

The lignin was then extracted in water and 1,4-dioxane (Sigma-Aldrich, ≥99 %) (15:85 v/v) solution acidified with HCl (Sigma-Aldrich, ACS reagent, 37 %) 10 mM under reflux at 86 °C for 2 h. Pulp lignin was also isolated using 50 mM HCl.

The spruce MWL was extracted according to Björkman (1956), but only the first purification step – dissolution in glacial acetic acid–water solution (Sigma-Aldrich, ≥99.7 %) (90:10) and precipitation in ultra-pure water – was performed.

To attain powders of similar properties and consistent loading of the DMA sample holder, the isolated lignins were solvent cast from methanol (Thermo Scientific, ≥99 %) and grounded in a mortar to a fine powder.

## 2.3 Kraft lignin fractionation

The fractionation of softwood kraft lignin was conducted according to Duval et al. (2016) – successive dissolution in small amounts of organic solvents (in the following order: ethyl acetate (Sigma-Aldrich, ≥99 %), ethanol (VWR, analytical grade), methanol (Thermo Scientific, ≥99 %), and acetone (VWR, analytical grade)) – which isolated fractions in different molecular-weight groups. The fractions used in this study have been characterized previously (Ghaffari et al. 2023).

## 2.4 Yield, purity and density

Combustion elemental analysis was conducted using a MICRO cube (Elementar, Germany), which quantifies the atomic content of C, H, N, and S. All samples were run in triplicates. Based on the N content, the protein contamination was calculated with a factor of 8, which is roughly the nitrogen factor of some cellulases (Kumar and Wyman 2008).

Ash content was determined using thermogravimetric analysis (TGA/DSC 3+ STAR System, Mettler Toledo, Switzerland) according to Aldaeus et al. (2017), Klason lignin contents of isolated lignin samples were assessed according to Aldaeus et al. (2011) and Klason lignin content of biomass was assessed according to Schwanninger and Hinterstoisser (2002). The acid-soluble lignin was determined with a Cary 60 UV–Vis spectrophotometer (Agilent Technologies Inc, USA) at 205 nm using the coefficient of 110 L/g cm. All analyses were done in duplicate.

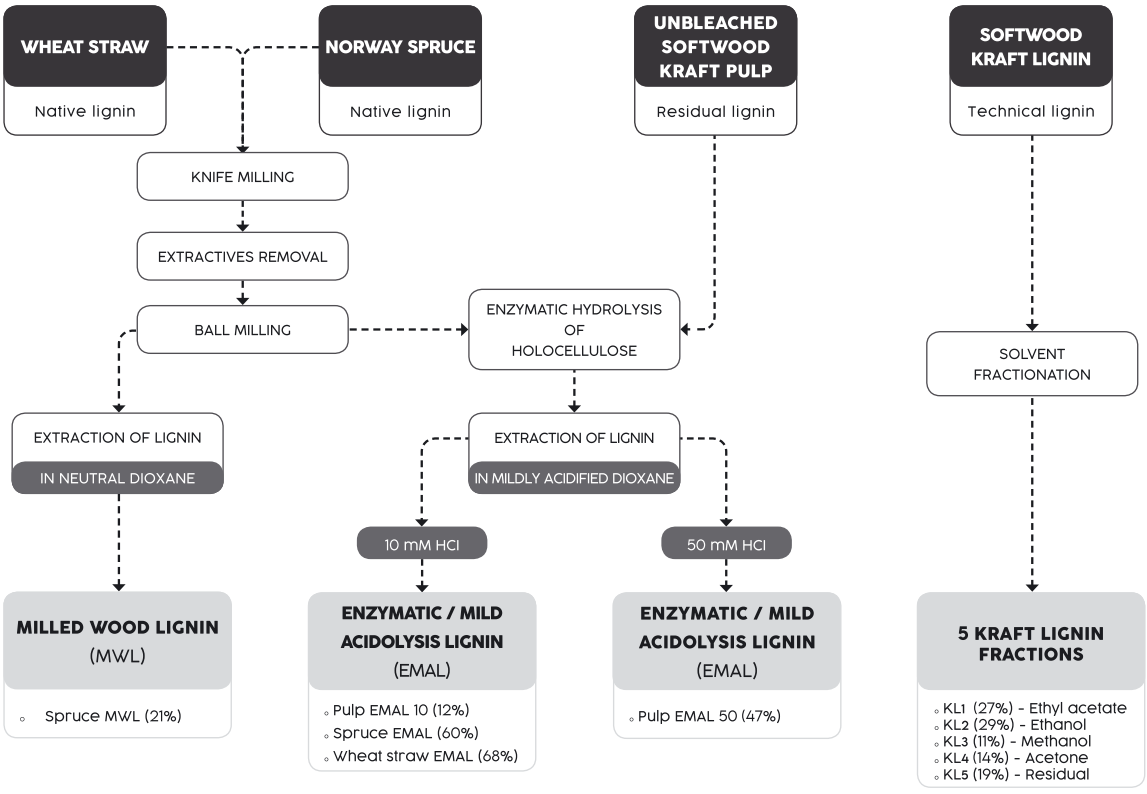


**Figure 1:** Flow chart of the isolation and fraction of lignin from various sources. The solvents used for the successive fractionation are specified for the given fraction. The yields of extraction are given in parentheses (wt/wt, see Table 1 for details).

True particle density was measured with a He Pycnometer (AccuPyc II 1340, Micromeritics, UK). As large sample sizes were needed, only the kraft lignin fractions were measured. The system was purged 10 times, and the apparent density was determined based on the average of the last five stable analysis cycles (relative standard deviation < 0.1 %). The samples were prepared just as for DMA.

## 2.5 Chemical structure analysis

A Spectrum One FTIR Spectrometer (PerkinElmer instruments, USA) fitted with an attenuated total reflectance (ATR) accessory was used to record Fourier transform IR (FTIR) spectra. Each material was measured with five replicates. The absorbance was recorded in the range of 4000–400 $cm^{-1}$ with 32 scans and a resolution of 4.0 $cm^{-1}$. The replicate spectra were mean averaged. The averaged spectra were then baseline-corrected using a moving-average smoothing algorithm and scaled with standard normal variate (SNV) in SpectraGryph 1.2.

$^{31}P$ nuclear magnetic resonance (NMR) quantification of hydroxyl groups was conducted according to Balakshin and Capanema (2015). A 1:1.6 solution of pyridine-$d_5$ (Sigma-Aldrich) and chloroform-$d_1$ (Chemtronica) was prepared. Standards of relaxation agent, chromium (III) acetylacetonate (Sigma-Aldrich) (11.4 mg/mL), and the internal standard (0.12 M), endo-*N*-hydroxy-5-norbornene-2,3-dicarboximide (Sigma-Aldrich), were prepared with the solvent solution. 40 mg of the sample was dissolved in 0.4 mL of the solvent solution, and 0.1 mL of the two standards were added. Finally, 0.1 mL of phosphorylation reagent, 2-chloro-4,4,5,5-tetramethyl-1,3,2-dioxaphospholane (Sigma-Aldrich), was added, and the flask tightly closed and vortexed for a few minutes. Measurements were conducted between 1 and 3 h after the addition of the reagent.

The solutions were transferred to 5 mm tubes, and the NMR spectra were recorded on a Bruker Avance 500 MHz utilizing inverse gate detection and a 90° pulse width. Acquisition and relaxation times were 1.0 and 5.0 s, respectively, and 256 scans were performed. The spectra were chemical shift calibrated using the anhydride product at 132.2 ppm. Baseline correction was done with a linear function. Unfractionated kraft lignin was run in duplicate with an average relative error of the quantified OH groups of 3.5 %, all other samples were measured once. The kraft lignin fractions were analyzed using the same method, but on a Bruker Avance III HD 400 MHz (Ghaffari et al. 2023).

## 2.6 Gel permeation chromatography (GPC) analysis

The molecular weights of the lignins were investigated with an L-GPC 50 Plus Integrated GPC system (Polymer Laboratories; Varian Inc., UK) equipped with two PolarGel-M columns (300 × 7.5 mm) and one PolarGel-M (50 × 7.5 mm) guard column. The system was run on dimethyl sulfoxide (DMSO, Sigma-Aldrich, >99.7 %) with 10 mM LiBr (Sigma-Aldrich, >99 %) at 0.5 mL/min and the temperature of 50 °C. Samples were prepared as follows: 10 mg of lignin was dissolved in 1 mL eluant solution, it was then diluted to a final concentration of 0.24 mg/mL and filtered with a 0.2 µm syringe filter. Samples were prepared in duplicates. An ultraviolet light detector scanning at 280 nm

was used. The data analysis was carried out using Cirrus GPC Software 3.2. A calibration curve was constructed from 9 pullulan standards (L2090-0100, Varian) spanning 800–0.3 kDa. Pullulan calibrations tend to undervalue the molecular weight of the lignins, as the hydrodynamic radius of lignins and pullulans in DMSO are not the same, but as the undervaluation is linear, comparisons can be made within the same series (Zinovyev et al. 2018). Based on the duplicates, the average relative error of all $M_n$ determinations was 1.8 %.

### 2.7 Thermal analysis

DMA measurements were conducted on a Q800 from TA instruments (USA) with a liquid nitrogen cooling system and a dual cantilever clamp with a powder holder (TA instruments). All measurements were conducted with a heating rate of 3 °C/min and an amplitude of 5 µm, within the linear viscoelastic region. All measurements were conducted from 20 °C to 50–70 °C above their $T_g$. Samples were run with a 5 min annealing at 120 °C to remove moisture. Measurements were done with a frequency of deformation of 1 Hz. All samples were run in triplicates. The steel powder holder contributes to the storage ($E'$) and loss ($E''$) moduli, but the steel doses do not have any transitions in the temperature range, thus, the transitions observed belong to the polymer in the sample holder. The $T_g$ was determined as the onset of the decline in $E'$ (the intersection of tangent lines from the glassy state and the glass transition, $T_{g\ E'\ \text{onset}}$), the maximum of the $E''$ ($T_{g\ E''\ \text{max}}$) and the maximum of the tan delta ($T_{g\ \text{tan delta max}}$). To facilitate comparison, the $E'$ values were normalized by division by its maximum value. Tan delta, defined as the ratio of $E''/E'$, is presented without modification.

DSC measurements were conducted on a DSC 2 STARe system instrument (Mettler Toledo, Switzerland) in 70 µL aluminum crucibles. All samples were run in triplicates of approximately 10 mg. The samples were subjected to two successive heating ramps from 25 °C to 50 °C above $T_g$ at 10 °C/min, with a 10 °C/min cooling ramp in between. The $T_g$ was determined in the second run at the inflection point.

## 3 Results and discussion

### 3.1 Yield, purity and molecular weight of lignins

To obtain lignins representative of their respective biomass, the high yield and purity protocol of EMAL was used for their extraction. EMAL lignin is isolated by ball milling, enzymatic hydrolysis of holocellulose and extraction in a mildly acidified dioxane-water solution. This method typically isolates more than half of the lignin but is still considered a mild method (Guerra et al. 2006a,b; Wu and Argyropoulos 2003). For the pulp sample, the milling is omitted, as the pulp is already separated into single fibers; however, higher acid concentrations are often needed (Argyropoulos et al. 2002; Jääskeläinen et al. 2003), likely due to the need to cleave the lignin-carbohydrate bonds that form during pulping (Lawoko et al. 2004). In this study, we used both a lower and a higher acid concentration for isolating pulp lignin (10 mM and 50 mM HCl, respectively), to compare the effect of acidity on yield and lignin structure. Spruce MWL was also prepared to include a lower-yield spruce lignin for comparison.

The amount of lignin extracted from the various sources, as well as the purity and molecular weight, are shown in Table 1. The yield of both EMAL and MWL reflects what is commonly found in the literature: EMAL between 40 % and 70 % and Spruce MWL of around 20–30 % (Björkman 1956; Guerra et al. 2006a,b; Jääskeläinen et al. 2003; Sun et al. 2005; Wu and Argyropoulos 2003). The Pulp EMAL isolated with 10 mM HCl resulted in a yield of 12 %; by increasing the HCl to 50 mM an isolation yield of 47 % was achieved.

The kraft lignin had the lowest molecular weight of the non-fractionated softwood lignins, whereas the pulp lignins had the largest, with the Spruce EMAL in-between. This follows from the extraction process of kraft cooking: the material that is extracted is cleaved and hydrolyzed into smaller pieces. The lignin that is left in the material either does not undergo reaction and solvation due to its high molecular weight, or it is mostly subjected to condensation reactions, which increase its molecular weight and insolubility (Balakshin et al. 2003).

The absolute yield of the softwood kraft lignin fractions was 77 %, meaning that 23 % was lost in the process, mainly during filtering. The yields based on the total retained material are shown in Table 1 and are similar to those of Duval et al. (2016) but with less material in the last insoluble fraction. As expected, the molecular weight of the fractions increases from KL1 to KL5 (Figure 2), and the dispersity ($Đ$) values are between 2 and 3. The true particle densities of the kraft lignin fractions were between 1.31 and 1.41 $10^{-3}$ kg/m$^3$.

All the EMALs have high number-average ($M_n$) and weight-average molecular weights ($M_w$), along with bimodal distributions. This bimodality has previously been found for EMALs in other chromatography setups (Guerra et al. 2006a,b; Jääskeläinen et al. 2003). In a study by Guerra et al. (2007), they found that aging acetobrominated EMAL in tetrahydrofuran (THF) at room temperature without stirring made the bimodality disappear. They proposed that the bimodality is due to self-association. To minimize any potential association, we performed an incubation in the eluent for 20 days, but no significant differences were detected from samples run after a few hours of their preparation (Figure S1). The eluent used in this study, DMSO with the addition of LiBr, deter association, but some self-association cannot be ruled out (Clauss et al. 2015; Ringena et al. 2006).

**Table 1:** Yield, molecular weight and purity of lignin samples extracted from biomass and of kraft lignin fractions (KL1-5).

| Sample name | Yield (%) | $M_n$ (kDa) | $M_w$ (kDa) | $Đ$ ($M_w/M_n$) | Purity[c] (%) | True particle density ($10^{-3}$ kg/m$^3$) |
|---|---|---|---|---|---|---|
| Spruce MWL | 21[a] | 2.8 | 7.2 | 2.6 | 95.2 (0.4) | – |
| Spruce EMAL | 60[a] | 3.8 | 27.5 | 7.3 | 92.6 (0.2) | – |
| Wheat straw EMAL | 68[a] | 3.1 | 15.7 | 5.0 | 93.2 (0.4) | – |
| Pulp EMAL 50 | 47[a] | 5.8 | 77.3 | 13.4 | 93.7 (0.1) | – |
| Pulp EMAL 10 | 12[a] | 4.7 | 37.0 | 7.9 | 90.3 (0.5) | – |
| Kraft lignin | – | 1.6 | 12.2 | 7.4 | 93.5 (0.6) | – |
| KL1 | 27[b] | 0.7 | 1.8 | 2.7 | – | 1.31 |
| KL2 | 29[b] | 1.9 | 5.4 | 2.9 | – | 1.39 |
| KL3 | 11[b] | 2.6 | 6.1 | 2.4 | – | 1.41 |
| KL4 | 14[b] | 6.8 | 13.4 | 2.0 | – | 1.34 |
| KL5 | 19[b] | 14.8 | 42.5 | 2.9 | – | 1.40 |

[a]Yield = mass of extract/mass of Klason and acid-soluble lignin of biomass. [b]Yield = mass of extract/sum of the mass of all fractions. [c]Purity = (Klason and acid-soluble lignin – ash content – protein contamination)/mass of the sample. Values in parentheses are the pooled standard deviations. See Table S1 for details.

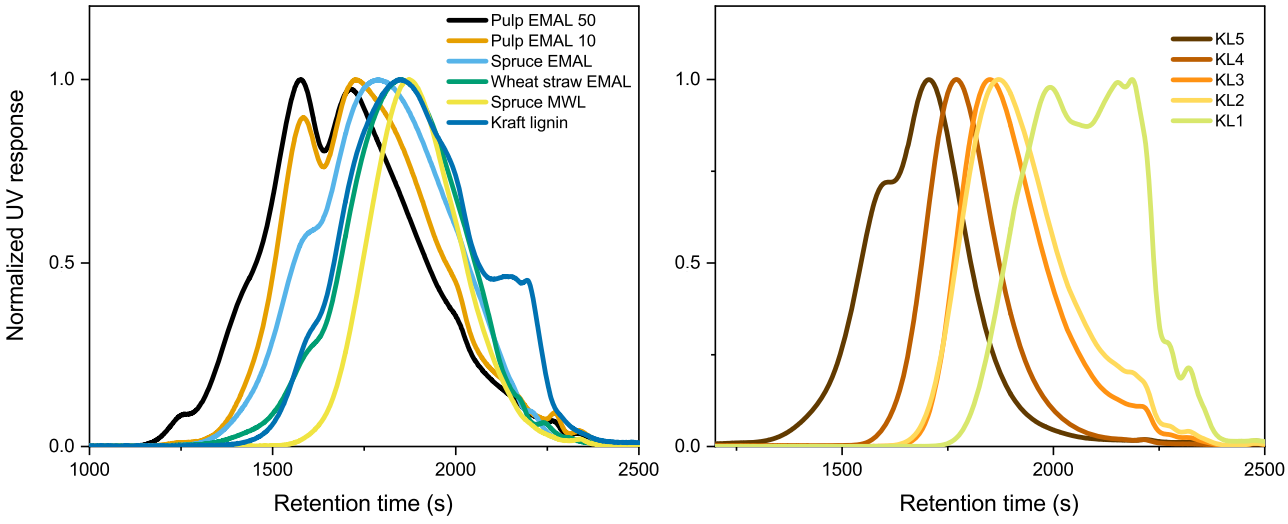


**Figure 2:** Min–max normalized GPC chromatograms of isolated lignins (left) and KL fractions (right).

## 3.2 Chemical structure

In this study, the difference between softwood and monocot, specifically Norway spruce and wheat straw, lies in both monomer content and internal linkages. This is confirmed in band shifts in both the vibrational spectra (Figure 3), as well as, by the $^{31}$P NMR analysis (Figure 4). Both wheat straw and softwood lignins contain guaiacyl (G) units, which are reflected in the FTIR spectra with peaks at 855 and 820 cm$^{-1}$. The presence of syringyl (S) units in wheat straw can be seen at 835 cm$^{-1}$, the C–H bending of S (Faix 1991; Sammons et al. 2013).

Wheat straw also contains many conjugated carbonyls, of which the flavonoid tricin and hydroxycinnamic acids make up a large part (del Río et al. 2012). Together with the acetyl and aldehydes groups of wheat straw lignin, as many as 15 conjugated carbonyls per 100 aromatic rings have been found (Zhang et al. 2022). This is reflected in the FTIR spectra, where Wheat straw EMAL has the most intense conjugated carbonyl stretching band at 1660 cm$^{-1}$ (Bock et al. 2020).

In this study, the axis ranging from Spruce MWL and EMAL to Pulp EMAL and kraft lignin represents the transition from more native to degraded; however, these differences are more subtle in the vibrational spectra. The spectra of Spruce MWL and Spruce EMAL and Pulp EMAL 10 and 50 were close to identical, and hence, only Spruce EMAL and Pulp EMAL 50 are shown in Figure 3. The IR band at 1330 and 1369 cm$^{-1}$ have been assigned to condensed lignin structures, such as 5-5 and other C5-substitutions

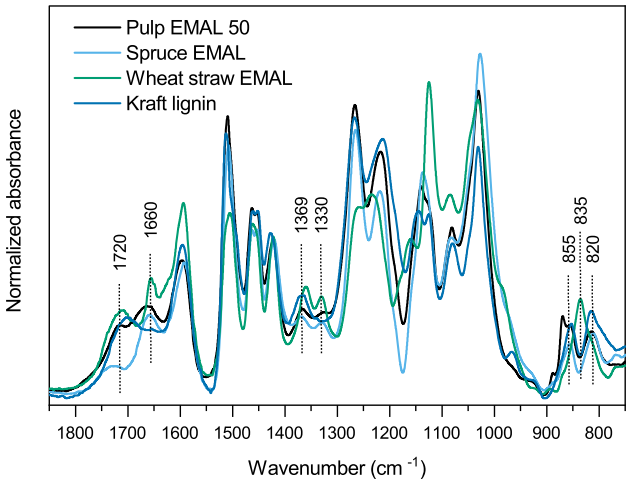


**Figure 3:** ATR-FTIR SNV normalized spectra. The peaks discussed in the text are indicated.

(Bock et al. 2020; Faix 1991), and both Pulp EMAL and kraft lignin have higher absorbance in the region, than the isolated native lignins. Likewise, FTIR confirms the presence of conjugated carbonyls (1660 $cm^{-1}$) in both Spruce EMAL and Pulp EMAL, but less so in kraft lignin, which indicates that the coniferyl aldehyde is intact in the former, but not the latter. The content of unconjugated carbonyls (1720 $cm^{-1}$) is higher in both kraft lignin and Pulp EMAL than in Spruce EMAL, which could indicate that new carbonyls have formed in both Pulp EMAL and kraft lignin due to oxidation.

In $^{31}P$ NMR of phosphorylated lignin, OH groups belonging to different structures can be quantified in relation to an internal standard. In Figure 4, the integration mode used, as suggested by Balakshin and Capanema (2015), to quantify the different structures is shown. Aliphatic, carboxylic and phenolic OH can be easily differentiated. Within the group of phenolics, C5-substituted (i.e., S and condensed G), non-condensed G ($G_{nc}$), and *p*-hydroxyphenyl (H) units can be differentiated. Softwood lignin only contains minimal amounts of S units, so the integral of C5-substituted compounds is primarily composed of condensed G units.

For wheat straw lignin, the picture is a bit more complex. Wheat straw lignin contains significant amounts of H, G, and S units, as well as the hydroxycinnamic acids of *p*-coumaric acid (pCA) and ferulic acid (FA) and the flavonoid tricin (Zhang et al. 2022). Tricin is believed to be an end group, and FA is a link to hemicelluloses. pCA is less likely to undergo radical coupling and should therefore exist as a side group with a free phenolic OH (Ralph et al. 2019). The OH groups of tricin have been assigned in a previous study and are annotated in Figure 4 (Heikkinen et al. 2014). pCA will appear in the H region, whereas FA, if there is any with free OH, would likely be found under $G_{nc}$. Tricin has only been found in monocot lignin (Li et al. 2016).

The integrated values for the isolated lignins can be seen in Figure 5. The isolated native lignins have high aliphatic OH content, and low phenolic and C5-substituted content, whereas the opposite is true for kraft lignin. The high phenolic OH content of kraft lignin reflects the cleavage of β-O-4. The low amount of aliphatic OH is due to the retroaldol reaction, in which the nucleophilic attack by hydroxide or bisulfide ion on the methide quinone leads to the loss of the aliphatic side chain (Crestini et al. 2017). The Pulp EMALs are intermediate in both aliphatic and

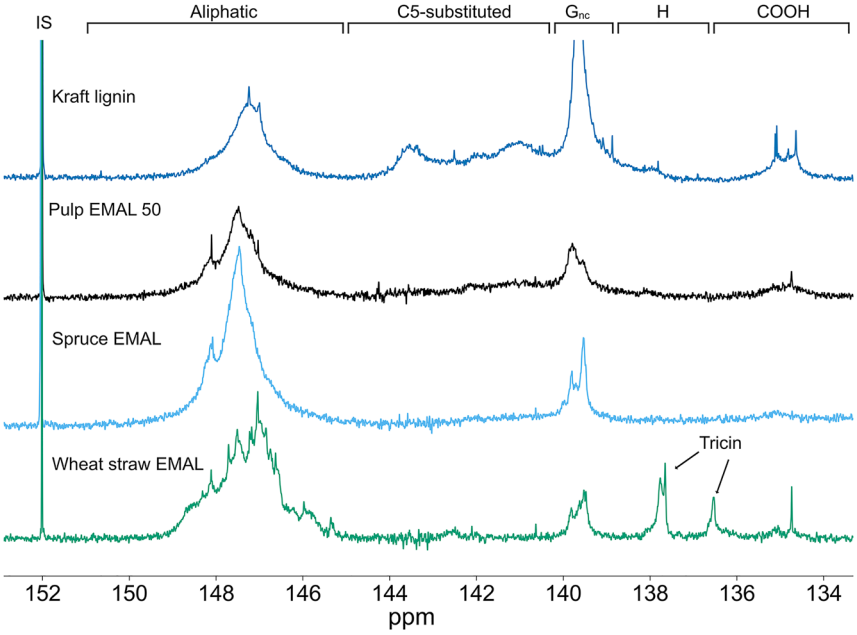


**Figure 4:** $^{31}P$ NMR spectra of selected lignins. Integration was done according to Balakshin and Capanema (2015). $G_{nc}$ is the integral of the non-condensed G unit and IS the internal standard. Tricin, present in monocot lignin, is marked in the spectrum of Wheat straw EMAL (Heikkinen et al. 2014).

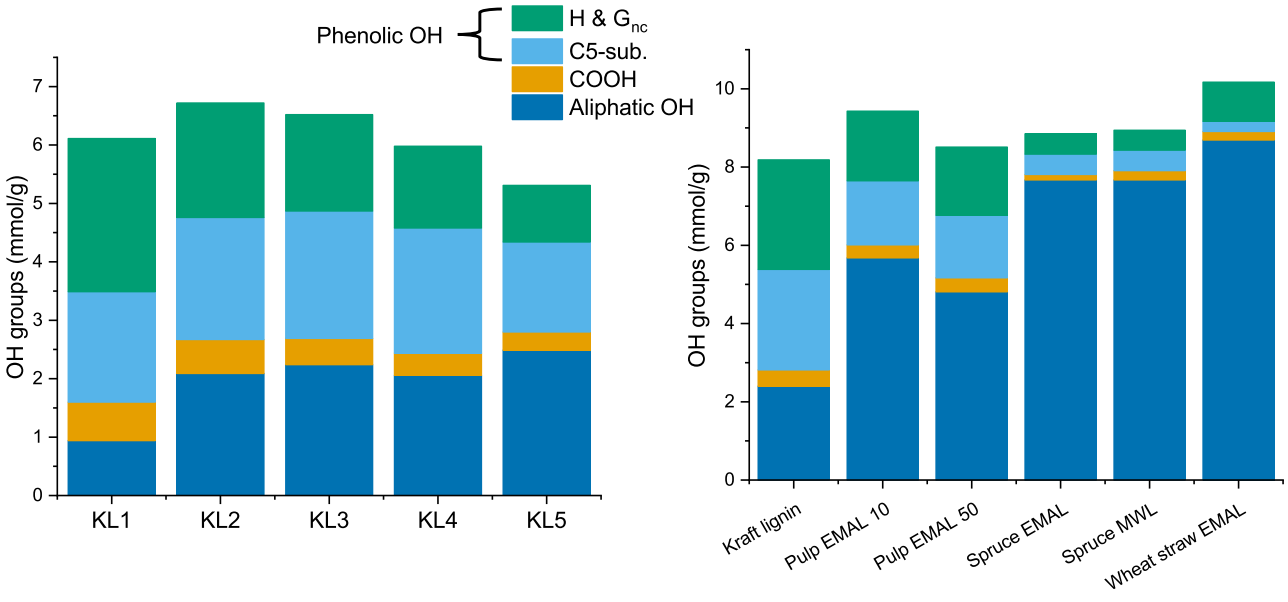


**Figure 5:** OH functional groups of kraft lignin fractions (left) and isolated lignins (right) determined with $^{31}$P NMR.

phenolic OH content, suggesting that they have been subjected to kraft pulping reactions to some degree. The structure of unbleached softwood kraft pulp lignin has previously been found to be an intermediary between native softwood lignin and kraft lignin (Balakshin et al. 2003).

New bonds are also formed during kraft pulping. This is reflected by the much higher content of C5-substituted phenolics for the softwood lignins that have undergone kraft pulping. These C5-substitutions are known to consist of 5-5 and 4-O-5 (Argyropoulos et al. 2021; Granata and Argyropoulos 1995), but others are likely possible. The residual lignin in pulp is also subjected to these condensation reactions, either with itself or with solubilized fractions, and it is believed to be one of the reasons why it has such high molecular weight (Majtnerová and Gellerstedt 2006).

The OH group content of Spruce MWL and Spruce EMAL are found to be very similar in this study. This suggests that EMAL has not undergone more aryl-ether cleavages or condensation reactions than MWL, and chemically it is a good representative of native lignin. Guerra et al. (2006a,b) made similar findings; they also found no or only a very slight significant difference in β-O-4 content between EMAL and MWL for several wood species.

The OH content of the fractionated lignins is relatively uniform, except for KL1 and KL5. KL1 has the highest phenol content of all, whereas KL5 appears to be more similar to the pulp lignins with lower C5-substitution and phenolic content and higher aliphatic OH. A detailed study has also reported the same trend on the same type of fractionated softwood kraft lignin (Gioia et al. 2018). It is thus clear that the solvent fractionation does not only isolate according to molecular weight but also due to chemical affinity.

## 3.3 DSC and DMA reproducibility

The only lignins in this study that gave clear and reproducible $T_g$ determinations with DSC were Spruce MWL and kraft lignin, and its fractions. The lignins of intermediate molecular weight, Spruce EMAL and Wheat straw EMAL, have the start of an endothermic event at around 170–200 °C, which was then obscured by an exotherm, preventing the formation of a baseline for determining the $T_g$ (Figure 6). The exothermic event is likely coupling reactions taking place at high temperatures (Moustaqim et al. 2018; Shrestha et al. 2017). The pulp lignins extracted with the EMAL protocol had no distinct endothermic transitions. The determination of the $T_g$ using DSC appears to be hindered by both the high molecular weight, which reduces the $\Delta C_p$ of polymers (Andreozzi et al. 2005; Wu et al. 2021), and the high dispersity in composition, causing a broadening of the transition. These factors, coupled with the previously mentioned exothermic reactions, collectively hinder the determination of $T_g$.

The powder sample holder for DMA gave clear $T_g$s for all lignins in the study (Figure 7). The precision of the two techniques can be seen in Figure 8 and Table S2. The curve profiles in Figure 7 are representative of the replications,

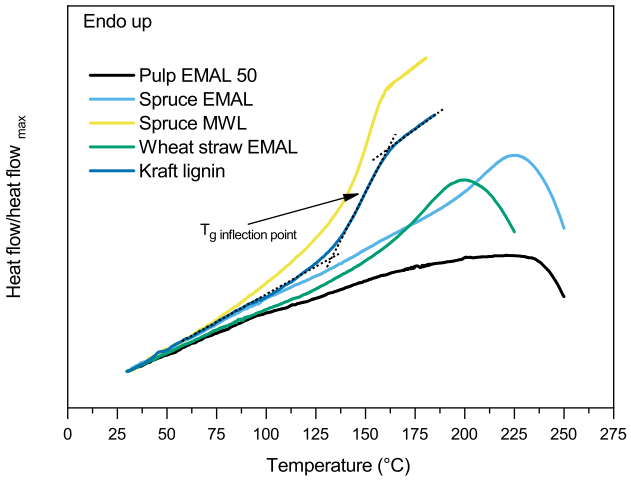


**Figure 6:** Max-normalized DSC graph of the second heat run at 10 °C/min. The $T_g$ determination by the point of inflection is illustrated for kraft lignin.

but to get a complete overview of the reproducibility, we refer to Figure S3 where replications have been collected. The $T_g$ determinations based on $E''$ maxima had smaller standard deviations compared to those based on $E'$ onset, especially for KL fractions with low $Đ$, likely due to the methodological ease of determining a maximum. The $E'$ onset of the transition is also more sensitive to aging effects, e.g., overshooting due to sudden stress relaxations (Menard 1999).

It should be noted that the annealing at 120 °C to remove moisture led to an increase in $T_g$ of about 5 °C. Whether this is due to water having left the system or condensation reactions is difficult to discern; however, no exothermic reactions were observed in the DSC thermograms under 200 °C. When kraft lignin and Spruce EMAL lignin were run without annealing but with two heat runs to 230 °C, a shift of the $T_g$ upwards of about 20 °C was observed between

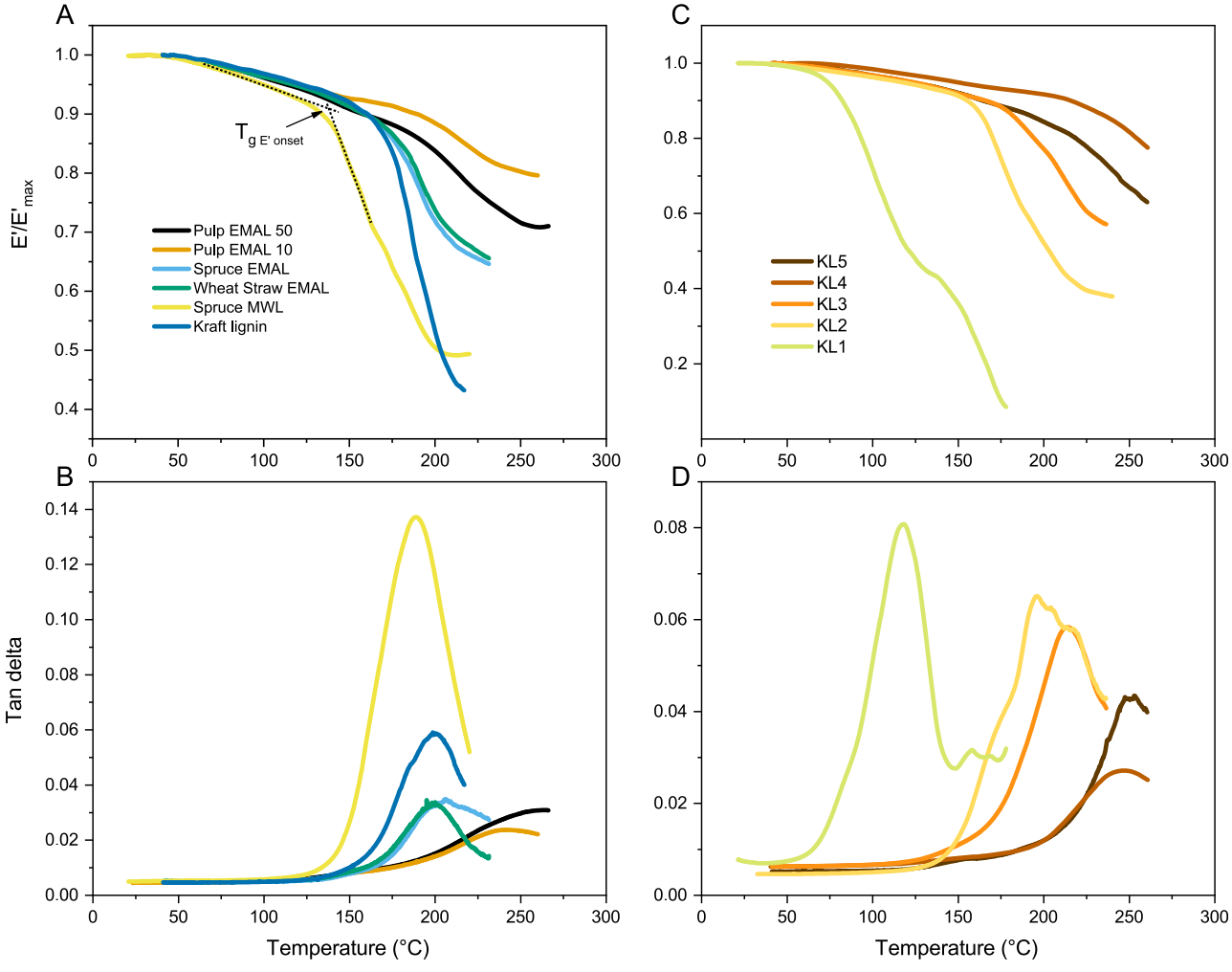


**Figure 7:** Thermograms of max-normalized $E'$ and tan delta. The unit of the storage modulus is Pascal (Pa), whereas the tan delta is unitless. The $T_g$ determination by the $E'$ onset is illustrated for Spruce MWL.

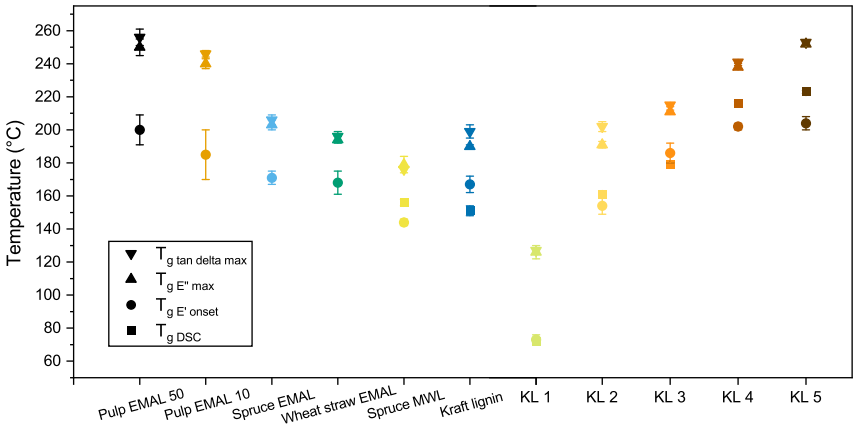


**Figure 8:** The $T_g$ determined with DSC and DMA. Inflection points in DCS ($T_g$) could only be reproducibly determined for Spruce MWL and softwood kraft lignin and its fractions (see Table S2 for values).

the first and the second run. It is evident that condensation reactions occur at elevated temperatures, which increases the $T_g$, as is often observed (Souto and Calado 2022). This will lead to a slight overestimation of the $T_g$ values of the high-$T_g$ samples in this study, but likely not more than 5–10 °C. As the $T_{g\ E'\ \mathrm{onset}}$ of all samples is below 205 °C, and therefore subjected to less condensation, these values will be used for modeling in the following section.

## 3.4 Influence of molecular weight and chemical structure

The effect of molecular weight on the $T_g$ of lignin is easily discernible when looking at the KL fractions (Figure 9). The $T_g$ increases rapidly with increasing molecular weight and then reaches a plateau. This Flory–Fox behavior of kraft lignin fractions has also been observed by other groups (Clauss et al. 2015; Ebrahimi Majdar et al. 2020; Sevastyanova et al. 2014). The Flory–Fox Equation (1) is an empirical relationship, which is interpreted with the theory of free volume: $M_n$ is a measure of the number of chain ends in a given volume, and chain ends have more free volume (Fox and Flory 1950; 1954). Ogawa (1992) offered a modification of the Flory–Fox Equation (2) that considers the molecular-weight dispersity. Ogawa did not offer any rationale for using the geometric mean, but higher $T_g$ values for polymers with high $Đ$ can be understood as that the longer chains will require more thermal energy to move (Gentekos et al. 2019).

$$T_g = T_{g,\infty} - \frac{K}{M_n} \quad (1)$$

$$T_g = T_{g,\infty} - \frac{K}{\sqrt{M_n M_w}} \quad (2)$$

where $T_{g,\infty}$ is the $T_g$ at infinitely high $M_n$, and $K$ is a constant that relates $M_n$ to $T_g$.

The $T_g$ was plotted against the reciprocal $M_n$ and $\sqrt{M_n M_w}$ to obtain linear relationships (Figure 9B and D). The $T_{g\ E'\ \mathrm{onset}}$ is sensitive to the width of the transition, which in turn is largely impacted by molecular weight dispersity and molecular composition, as will be elaborated on below. Although $T_{g\ E''\ \mathrm{max}}$, positioned at the transition's centre, might offer better $T_g$ modelling, our choice was $T_{g\ E'\ \mathrm{onset}}$, as discussed earlier, to avoid degradation effects. Nevertheless, similar correlations were found using $T_{g\ E''\ \mathrm{max}}$. The Flory–Fox and Ogawa equations are here used to study how the isolated lignins relate to each other and the kraft lignin fractions. The two constants of the equation ($T_{g,\infty}$ and $K$) are related to the free volume of the polymer but can be understood in a more general way, as describing the stiffness of the polymers and the strength of the interactions between polymer chains – higher values correspond to stiffer chains or stronger secondary interactions or both (Boyer 1974).

The KL fractions were fitted with a line in the Flory-Fox and Ogawa plots (Figure 9B and D) with coefficients of determination of 0.972 and 0.947, respectively. The goodness of fit is likely suffering from the chemical heterogeneity of the samples – i.e. it is not only the molecular weight that is shifting. KL1 has a large impact on the fit due to its separation from the other points. Fitting the line without KL1 shifts the slope slightly but does not change the interpretation of the data. As discussed earlier, the molecular weights are also undervalued when determined with pullulan standards (Zinovyev et al. 2018), but the undervaluation is linear, which allows for comparison; still, it does not allow for correct determinations of the $K$ and $T_{g,\infty}$ constants. It is however clear that a Flory–Fox equation for softwood kraft lignin determined with correct molecular weights, would have a $T_{g,\infty}$ over 200 °C which is indicative of a stiff and strongly interacting polymer system.

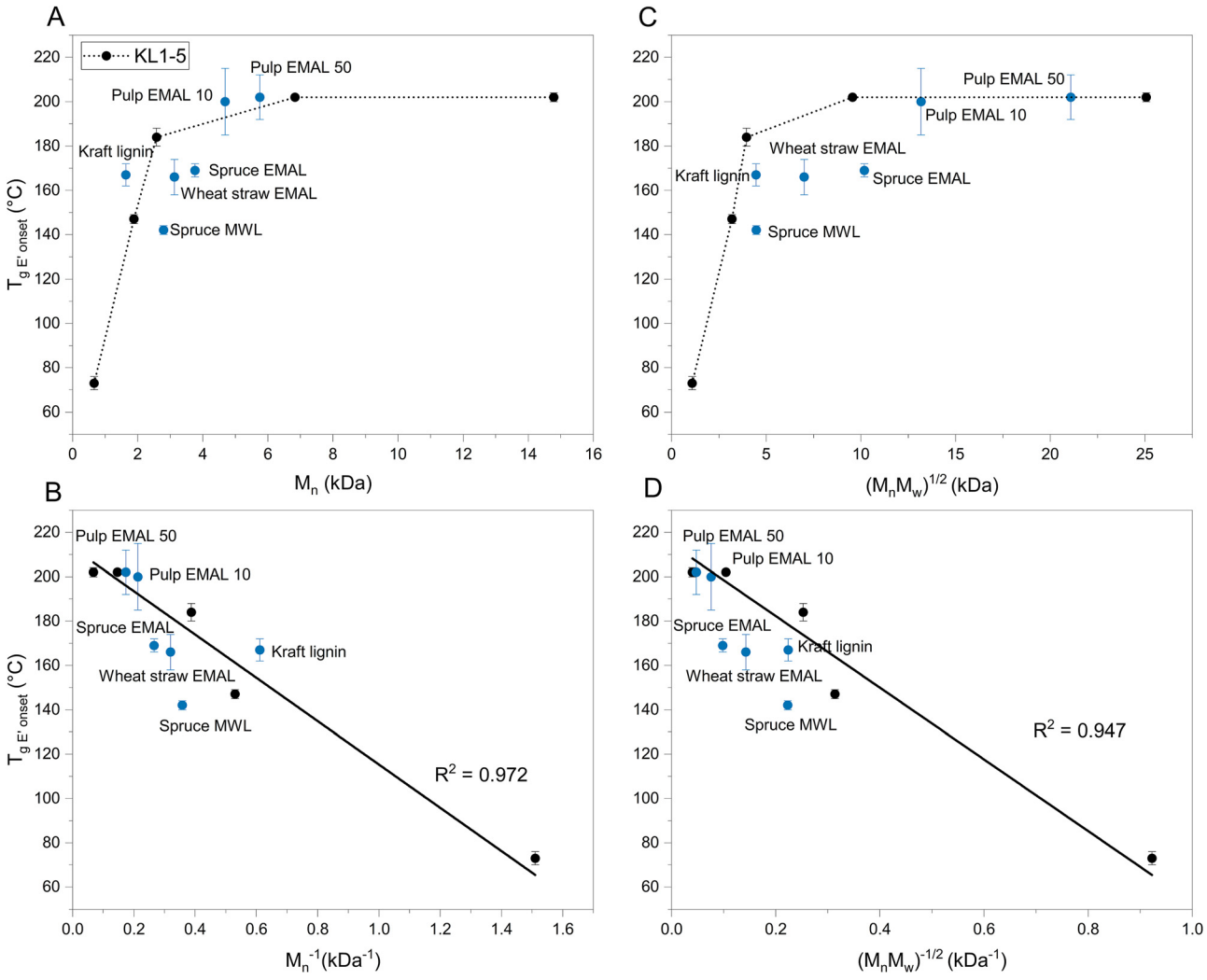


**Figure 9:** Flory–Fox (A and B) and Ogawa (C and D) plots. The kraft lignin fractions (black) have been fitted with a linear regression in the reciprocal plots, whereas the dotted lines in the top plots are for guidance.

In the Flory–Fox and Ogawa plots (Figure 9B and D), the isolated native lignins are positioned below the fitted line, suggesting a less stiff polymer. This agrees with the higher degree of flexible β-O-4 linkages in native lignin as compared to kraft lignin. The isolated pulp lignins are positioned slightly above the linear regression in the Flory–Fox plot, which is surprising, as the pulp lignins are less condensed than the kraft lignins. The Ogawa plot (Figure 9D), which takes better account of molecular-weight dispersity, has the pulp lignins on the fitted line. This would suggest that the pulp lignins actually have flexibility more similar to that of the kraft lignins, but their very high $Đ$ obscures this correlation in the Flory–Fox plot.

The proximity of Pulp EMAL and kraft lignin in the Ogawa plot is still unexpected, as Pulp EMAL has a structure intermediate between native and technical lignin and would be expected to exhibit an intermediate $T_{g,\infty}$. However, many factors affect the $T_g$ of polymers. The hypothesis that phenolic OH partakes in less hydrogen bonding than aliphatic OH (Kubo and Kadla 2005), could help explain the unexpected result. The higher phenol content of kraft lignin depressed the $T_g$ of the rigid, condensed chains, while the high $T_g$ of the less rigid and condensed Pulp EMAL could be attributed to its higher alcohol content.

Another factor to consider is the branching of lignins. It remains a debated issue whether native lignin is branched or not (Balakshin et al. 2020; Crestini et al. 2011; Ralph et al. 2019; Sapouna and Lawoko 2021), but technical kraft lignins exhibit branching attributed to coupling reactions occurring during kraft pulping (Crestini et al. 2017). Branching in polymers introduces both stiffness, by restricting segmental movements, and mobility, by increasing the amount of

mobile chain ends (Khalyavina et al. 2012); thus, the net effect of branched chains on the $T_g$ of a given polymer system is not easily established. If the net effect of branching in kraft lignin is depressing the $T_g$, a similar hypothesis as in the paragraph above could be formulated –the stiff chains of kraft lignin are counterbalanced by the increase in free volume by the many chain ends of its branches.

In addition to the $T_g$, Figure 7 also provides information on the width of the glass transition. All the lignins exhibit wide glass transitions, with most samples spanning over 100 °C in tan delta, which is larger than what is typically found for synthetic polymers. In synthetic polymers, broad glass transitions are found when the material contains a wide range of nanoscale compositional variations, typically seen in certain kinds of copolymers (gradient copolymers) or polymer blends (Mok et al. 2008). With the heterogenous composition and structure of most lignins, it seems reasonable to assume that their transitional width is due to the same kind of variating nanodomains. As the processing of thermoplastics is done at a temperature beyond the $T_g$, the breadth of the transition poses another obstacle, together with the high $T_g$, to lignin thermoforming; however, in some applications, such as acoustic and vibrational damping, broad glass transitions are desirable (Alam et al. 2019).

The $E'$ and $E''$ determined using the powder sample holder are non-absolute as the geometry factor for powders is not known and as straining the steel sample holder contributes to the signal. The question is whether any relative comparisons can be made based on the moduli values. The same geometry factor and sample size were maintained for all samples in all measurements. The factors that could then affect the magnitude of the moduli are the packing conditions and the material itself. To achieve similar packing conditions, all lignins were solvent cast, ground in a mortar, spread out evenly in the sample holder and clamped to avoid particle movements. For the kraft lignin fractions, the moduli values correlate to molecular weight, but not to the density, which supports the claim that relative differences in modulus are due to differences in polymer chain movements.

The dynamic mechanical properties of polymers in the glassy state are not greatly affected by molecular weight, as the molecular movements are limited. In the rubbery state, however, the length of the polymer chains greatly affects their movement and, hence, the viscoelastic properties of the material (Ward and Sweeney 2004). This behavior can be seen in the KL fractions: similar amounts of force are needed to deform KL1-5 before the $T_g$, but the magnitude of the drop in $E'$ over the glass transition decreases drastically with increasing molecular weight. The tan delta also shows that the dissipation of energy by polymer movements is much greater in low-molecular-weight fractions. This trend has been found previously (Karaaslan et al. 2021; Sevastyanova et al. 2014). KL5 is the exception as it consistently has a larger drop in $E'$ than KL4, even though the molecular weight is much higher. This could be because KL5 appears to have gone through fewer kraft pulping reactions – it has a higher aliphatic OH content and less condensed groups – and thus retains more flexibility.

KL1 is the only lignin in the study that started to flow out of the pocket during the measurement. KL1 has a drop in $E'$ at 73 °C, followed by another drop at around 120 °C. Just before the second drop, the displacement reading of the instrument falls rapidly. It would then appear as if the first drop is the glass transition to the rubbery state and the second drop is the transition to a viscous flow. These measurements were conducted without annealing.

The isolated lignins in Figure 7 follow the same pattern as the KL fractions. The lower molecular-weight kraft lignin and Spruce MWL have a large drop in $E'$, the intermediary Spruce EMAL and Wheat straw EMAL fall in the middle, and the very high molecular-weight Pulp EMALs have a small drop in $E'$. The large discrepancy in structure between the different lignins appears less important than their molecular weight when it comes to their thermal softening.

Spruce EMAL would appear to be a better representative of native lignin than Spruce MWL as it contains 60 % of the lignin in spruce, compared to 21 % for Spruce MWL. This is also reflected in the fact that Spruce EMAL, with a $T_{g\,E''\,\max}$ slightly over 200 °C, is closer to the values found for dry softwood determined in the same way (Startsev et al. 2017). Both Spruce MWL and Spruce EMAL were ball milled, and it is known that ball milling depolymerizes lignin to some extent. In a recent study, evidence was found that ball milling mainly depolymerizes lignin far from cellulose (Sapouna and Lawoko 2021). This could also help describe the difference between Spruce MWL and Spruce EMAL: without enzymatic and acidic hydrolysis of the carbohydrate matrix, mainly depolymerized, and possibly, slightly more condensed lignin is isolated.

A problem inherent in the EMAL protocol, concerning representativity, is the lignin-carbohydrate complexes (LLC). As both the LCC linkages and the carbohydrate chains themselves are hydrolyzed to a large extent, a fundamental aspect of both native and residual lignin is lost. Some LCC linkages in MWL and EMAL lignins have been found to be retained upon isolation (~10 LLC linkages/100 aromatic units) (Yuan et al. 2011), but the carbohydrate chains were so short that they likely only had a small effect in this study.

Another difference between *in situ* and isolated lignin is the morphology of the polymer. It is known that interfaces of polymers are more confined than the bulk if the polymer has strong interactions with the substrate, which leads to a

local increase in $T_g$ (Napolitano et al. 2017). Lignin in the secondary cell wall is polymerized into nanometer spaces, and, thus, has a large surface-to-bulk ratio. There is evidence that lignin in the cell wall has specific conformations, as it maximizes its interactions with itself and its surroundings (Kang et al. 2019; Terashima et al. 2009; Vural et al. 2018). Based on these findings, one could suspect that lignin is highly confined in the cell wall and has less flexibility than isolated lignin and, consequently, a higher $T_g$.

Monocot Wheat straw EMAL and softwood Spruce EMAL appear very similar in both $T_g$ and DMA curve profiles. In the Flory–Fox plot, a straight line could almost be drawn between Spruce MWL, Wheat straw EMAL and Spruce EMAL, which indicates a similar relationship between $T_g$ and $M_n$. This clashes with the general conception that S-containing lignin is more dynamic and generally has a lower $T_g$ (Olsson and Salmén 1997; Vural et al. 2018). The reason for this might be the bulky pCA side groups and the tricin end group, which likely add to the stiffness of wheat straw lignin. Wheat straw EMAL also had the highest amount of OH groups of all the lignins, with 1.5 mmol/g more than the spruce lignins, which could also have contributed to the stiffness and counterbalanced the dynamic S unit.

# 4 Conclusions

By isolating lignin in high yield from Norway spruce and softwood kraft pulp, and by fractionating softwood kraft lignin, and subjecting them to DMA, a detailed thermo-mechanical analysis of the transformation from native to processed lignin was possible. A comparative analysis of stiffness independent of molecular weight was possible by applying the Flory–Fox and Ogawa equations to model the $T_g$. The models indicated that softwood kraft lignin and softwood kraft pulp lignin have similar flexibility, whereas native lignin appeared to be more flexible. Employing this approach to investigate variations in $T_g$, yields more comprehensive insights than the binary comparisons commonly used in the examination of residual pulp lignin.

Softwood residual pulp lignin has the highest $T_g$ and the lowest degree of thermal softening of all the lignins due to the combination of high molecular weight and relatively high degree of condensation. These poor thermoplastic properties suggest that molding lignin-containing kraft pulp requires refined plasticization techniques. Apart from external and internal plasticization, our study points towards depolymerization as an effective measure to enhance the flow properties of lignin. Even if condensation reactions take place alongside depolymerization (as is often the case for lignin), as long as the net result leads to a reduction in molecular weight, a subsequent decline in $E'$ in the rubbery region is expected.

Finally, the EMAL protocol isolated 60 % of the lignin from Norway spruce, which was found to have a $T_g$ more similar to what has been found for *in situ* lignin in softwood (Startsev et al. 2017), which advocates for it being a better representative of native lignin than MWL. Likewise, the Pulp EMAL isolated had a $T_g$ in the same range as the softening temperature of kraft pulp (Salmén and Back 1978), which would advocate for its representativity. However, EMAL isolates very small amounts of LCC. To further understand the structure-property relationship of lignin, it is necessary to study lignin isolated with intact LCC.

**Acknowledgments:** We thank Professor Lars Wågberg and Professor Gunnar Henriksson for their contribution in discussing lignin isolation.
**Research ethics:** Not applicable.
**Author contributions:** The authors have accepted responsibility for the entire content of this manuscript and approved its submission.
**Competing interests:** The authors state no conflict of interest.
**Research funding:** This research was funded by FibRe - a Vinnova-funded Competence Centre for Design for Circularity: Lignocellulose-based Thermoplastics (grant no. 2019-00047). F.C. and L.O. acknowledge support from the Swedish Energy Agency (grant no. 2019-021473). L.O., A.L. and R.G. acknowledge support from Wallenberg Wood Science Center.
**Data availability:** The raw data can be obtained on request from the corresponding author.

# References

Alam, M.M., Jack, K.S., Hill, D.J.T., Whittaker, A.K., and Peng, H. (2019). Gradient copolymers – preparation, properties and practice. *Eur. Polym. J.* 116: 394–414.

Aldaeus, F., Schweinebarth, H., Törngren, P., and Jacobs, A. (2011). Simplified determination of total lignin content in kraft lignin samples and black liquors. *Holzforschung* 65: 601–604.

Aldaeus, F., Olsson, A.-M., and Stevanic, J.S. (2017). Miniaturized determination of ash content in kraft lignin samples using oxidative thermogravimetric analysis. *Nord. Pulp Pap. Res. J.* 32: 280–282.

Andreozzi, L., Faetti, M., Giordano, M., and Zulli, F. (2005). Molecular-weight dependence of enthalpy relaxation of PMMA. *Macromolecules* 38: 6056–6067.

Argyropoulos, D.S., Sun, Y., and Palus, E. (2002). Isolation of residual kraft lignin in high yield and purity. *TAPPI J.* 28: 50–54.

Argyropoulos, D.S., Pajer, N., and Crestini, C. (2021). Quantitative 31P NMR analysis of lignins and tannins. *J. Visualized Exp.*: e62696, https://doi.org/10.3791/62696-v.

Ashaduzzaman, M., Hale, M.D., Ormondroyd, G.A., and Spear, M.J. (2020). Dynamic mechanical analysis of Scots pine and three tropical hardwoods. *Int. Wood Prod. J.* 11: 189–203.

Back, E. and Salmén, L. (1982). Glass transitions of wood components hold implications for molding and pulping processes. *TAPPI J.* 65: 107–110.

Balakshin, M. and Capanema, E.A. (2015). On the quantification of lignin hydroxyl groups with 31P and 13C NMR spectroscopy. *J. Wood Chem. Technol.* 35: 220–237.

Balakshin, M., Capanema, E.A., Zhu, X., Sulaeva, I., Potthast, A., Rosenau, T., and Rojas, O.J. (2020). Spruce milled wood lignin: linear, branched or cross-linked? *Green Chem.* 22: 3985–4001.

Balakshin, M.Y., Capanema, E.A., and ChenGracz, H.S. (2003). Elucidation of the structures of residual and dissolved pine kraft lignins using an HMQC NMR technique. *J. Agric. Food Chem.* 51: 6116–6127.

Björkman, A. (1956). Studies on finely divided wood. Part 1. Extraction of lignin with neutral solvents. *Sven. Papperstidn.* 59: 477–485.

Bock, P., Nousiainen, P., Elder, T., Blaukopf, M., Amer, H., Zirbs, R., Potthast, A., and Gierlinger, N. (2020). Infrared and Raman spectra of lignin substructures: dibenzodioxocin. *J. Raman Spectrosc.* 51: 422–431.

Boyer, R.F. (1974). Variation of polymer glass temperatures with molecular weight. *Macromolecules* 7: 142–143.

Clauss, M.M., Weldin, D.L., Frank, E., Giebel, E., and Buchmeiser, M.R. (2015). Size-exclusion chromatography and aggregation studies of acetylated lignins in N,N-dimethylacetamide in the presence of salts. *Macromol. Chem. Phys.* 216: 2012–2019.

Crestini, C., Melone, F., Sette, M., and Saladino, R. (2011). Milled wood lignin: a linear oligomer. *Biomacromolecules* 12: 3928–3935.

Crestini, C., Lange, H., Sette, M., and Argyropoulos, D.S. (2017). On the structure of softwood kraft lignin. *Green Chem.* 19: 4104–4121.

Del Río, J.C., Rencoret, J., Prinsen, P., Martínez, Á.T., Ralph, J., and Gutiérrez, A. (2012). Structural characterization of wheat straw lignin as revealed by analytical pyrolysis, 2D-NMR, and reductive cleavage methods. *J. Agric. Food Chem.* 60: 5922–5935.

Du, X., Gellerstedt, G., and Li, J. (2013). Universal fractionation of lignin–carbohydrate complexes (LCCs) from lignocellulosic biomass: an example using spruce wood. *Plant J.* 74: 328–338.

Duval, A., Vilaplana, F., Crestini, C., and Lawoko, M. (2016). Solvent screening for the fractionation of industrial kraft lignin. *Holzforschung* 70: 11–20.

Ebrahimi Majdar, R., Ghasemian, A., Resalati, H., Saraeian, A., Crestini, C., and Lange, H. (2020). Case study in kraft Lignin fractionation: "structurally purified" lignin fractions: the role of solvent H-bonding affinity. *ACS Sustain. Chem. Eng.* 8: 16803–16813.

El Hage, R., Brosse, N., Sannigrahi, P., and Ragauskas, A. (2010). Effects of process severity on the chemical structure of Miscanthus ethanol organosolv lignin. *Polym. Degrad. Stab.* 95: 997–1003.

Faix, O. (1991). Classification of lignins from different botanical origins by FT-IR spectroscopy. *Holzforschung* 45: 21–27.

Fox, S.C. and McDonald, A.G. (2010). Chemical and thermal characterization of three industrial lignins and their corresponding lignin esters. *BioResources* 5: 990–1009.

Fox, T.G., Jr. and Flory, P.J. (1950). Second-order transition temperatures and related properties of polystyrene. I. Influence of molecular weight. *J. Appl. Phys.* 21: 581–591.

Fox, T.G. and Flory, P.J. (1954). The glass temperature and related properties of polystyrene. Influence of molecular weight. *J. Polym. Sci.* 14: 315–319.

Gentekos, D.T., Sifri, R.J., and Fors, B.P. (2019). Controlling polymer properties through the shape of the molecular-weight distribution. *Nat. Rev. Mater.* 4: 761–774.

Ghaffari, R., Almqvist, H., Idström, A., Sapouna, I., Evenäs, L., Lidén, G., Lawoko, M., and Larsson, A. (2023). Effect of alkalinity on the diffusion of solvent-fractionated lignin through cellulose membranes. *Cellulose* 30: 3685–3698.

Ghose, T.K. (1987). Measurement of cellulase activities. *Pure Appl. Chem.* 59: 257–268.

Gioia, C., Lo Re, G., Lawoko, M., and Berglund, L. (2018). Tunable thermosetting epoxies based on fractionated and well-characterized lignins. *J. Am. Chem. Soc.* 140: 4054–4061.

Giummarella, N., Zhang, L., Henriksson, G., and Lawoko, M. (2016). Structural features of mildly fractionated lignin carbohydrate complexes (LCC) from spruce. *RSC Adv.* 6: 42120–42131.

Giummarella, N., Pu, Y., Ragauskas, A.J., and Lawoko, M. (2019). A critical review on the analysis of lignin carbohydrate bonds. *Green Chem.* 21: 1573–1595.

Goring, D.A.I. (1963). Thermal softening of lignin, hemicellulose and cellulose. *Pulp Pap. Mag. Can.* 64: T517–T527.

Granata, A. and Argyropoulos, D.S. (1995). 2-Chloro-4,4,5,5-tetramethyl-1,3,2-dioxaphospholane, a reagent for the accurate determination of the uncondensed and condensed phenolic moieties in lignins. *J. Agric. Food Chem.* 43: 1538–1544.

Guerra, A., Filpponen, I., Lucia, L.A., and Argyropoulos, D.S. (2006a). Comparative evaluation of three lignin isolation protocols for various wood species. *J. Agric. Food Chem.* 54: 9696–9705.

Guerra, A., Filpponen, I., Lucia, L.A., Saquing, C., Baumberger, S., and Argyropoulos, D.S. (2006b). Toward a better understanding of the lignin isolation process from wood. *J. Agric. Food Chem.* 54: 5939–5947.

Guerra, A., Gaspar, A.R., Contreras, S., Lucia, L.A., Crestini, C., and Argyropoulos, D.S. (2007). On the propensity of lignin to associate: a size exclusion chromatography study with lignin derivatives isolated from different plant species. *Phytochemistry* 68: 2570–2583.

Hatakeyama, H. and Hatakeyama, T. (2010) Thermal properties of isolated and in situ lignin. In: Heitner, C., Dimmel, D., and Schmidt, J.A. (Eds.). *Lignin and lignans : advances in chemistry*. CRC Press, Boca Raton, pp. 301–319.

Havimo, M. (2009). A literature-based study on the loss tangent of wood in connection with mechanical pulping. *Wood Sci. Technol.* 43: 627–642.

Heikkinen, H., Elder, T., Maaheimo, H., Rovio, S., Rahikainen, J., Kruus, K., and Tamminen, T. (2014). Impact of steam explosion on the wheat straw lignin structure studied by solution-state nuclear magnetic resonance and density functional methods. *J. Agric. Food Chem.* 62: 10437–10444.

Heitner, C. and Atack, D. (1984). Dynamic mechanical properties of sulphite treated aspen. *PAP PUU* 66: 84–89.

Jääskeläinen, A.S., Sun, Y., Argyropoulos, D.S., Tamminen, T., and Hortling, B. (2003). The effect of isolation method on the chemical structure of residual lignin. *Wood Sci. Technol.* 37: 91–102.

Kang, X., Kirui, A., Dickwella Widanage, M.C., Mentink-Vigier, F., Cosgrove, D.J., and Wang, T. (2019). Lignin-polysaccharide interactions in plant secondary cell walls revealed by solid-state NMR. *Nat. Commun.* 10: 347.

Karaaslan, M.A., Cho, M., Liu, L.-Y., Wang, H., and Renneckar, S. (2021). Refining the properties of softwood kraft lignin with acetone: effect of solvent fractionation on the thermomechanical behavior of electrospun fibers. *ACS Sustain. Chem. Eng.* 9: 458–470.

Karlsson, M., Romson, J., Elder, T., Emmer, Å., and Lawoko, M. (2023). Lignin structure and reactivity in the organosolv process studied by NMR spectroscopy, mass spectrometry, and density functional theory. *Biomacromolecules* 24: 2314–2326.

Kelley, S.S., Rials, T.G., and Glasser, W.G. (1987). Relaxation behaviour of the amorphous components of wood. *J. Mater. Sci.* 22: 617–624.

Khalyavina, A., Häußler, L., and Lederer, A. (2012). Effect of the degree of branching on the glass transition temperature of polyesters. *Polymer* 53: 1049–1053.

Kubo, S. and Kadla, J.F. (2005). Hydrogen bonding in lignin: a Fourier transform infrared model compound study. *Biomacromolecules* 6: 2815–2821.

Kumar, R. and Wyman, C.E. (2008). An improved method to directly estimate cellulase adsorption on biomass solids. *Enzyme Microb. Technol.* 42: 426–433.

Lawoko, M., Berggren, R., Berthold, F., Henriksson, G., and Gellerstedt, G. (2004). Changes in the lignin-carbohydrate complex in softwood kraft pulp during kraft and oxygen delignification. *Holzforschung* 58: 603–610.

Li, H. and McDonald, A.G. (2014). Fractionation and characterization of industrial lignins. *Ind. Crops Prod.* 62: 67–76.

Li, M., Pu, Y., Yoo, C.G., and Ragauskas, A.J. (2016). The occurrence of tricin and its derivatives in plants. *Green Chem.* 18: 1439–1454.

Mahlin, D., Wood, J., Hawkins, N., Mahey, J., and Royall, P.G. (2009). A novel powder sample holder for the determination of glass transition temperatures by DMA. *Int. J. Pharm.* 371: 120–125.

Majtnerová, A. and Gellerstedt, G. (2006). Radical coupling – a major obstacle to delignification in kraft pulping. *Nord. Pulp Pap. Res. J.* 21: 129–134.

Menard, K.P. (1999). *Dynamic mechanical analysis: a practical introduction*. CRC Press, Boca Raton.

Mok, M.M., Kim, J., and Torkelson, J.M. (2008). Gradient copolymers with broad glass transition temperature regions: design of purely interphase compositions for damping applications. *J. Polym. Sci., Part B: Polym. Phys.* 46: 48–58.

Moustaqim, M.E., Kaihal, A.E., Marouani, M.E., Men-La-Yakhaf, S., Taibi, M., Sebbahi, S., Hajjaji, S.E., and Kifani-Sahban, F. (2018). Thermal and thermomechanical analyses of lignin. *Sustainable Chem. Pharm.* 9: 63–68.

Napolitano, S., Glynos, E., and Tito, N.B. (2017). Glass transition of polymers in bulk, confined geometries, and near interfaces. *Rep. Prog. Phys.* 80: 036602.

Novy, V., Nielsen, F., Cullen, D., Sabat, G., Houtman, C.J., and Hunt, C.G. (2021). The characteristics of insoluble softwood substrates affect fungal morphology, secretome composition, and hydrolytic efficiency of enzymes produced by Trichoderma reesei. *Biotechnol. Biofuels* 105: 1–17.

Ogawa, T. (1992). Effects of molecular weight on mechanical properties of polypropylene. *J. Appl. Polym. Sci.* 44: 1869–1871.

Olsson, A.-M. and Salmén, L. (1997). The effect of lignin composition on the viscoelastic properties of wood. *Nord. Pulp Pap. Res. J.* 12: 140–144.

Pan, X.-J. and Sano, Y. (2000). Comparison of acetic acid lignin with milled wood and alkaline lignins from wheat straw. *Holzforschung* 54: 61–65.

Ralph, J., Lapierre, C., and Boerjan, W. (2019). Lignin structure and its engineering. *Curr. Opin. Biotechnol.* 56: 240–249.

Ringena, O., Lebioda, S., Lehnen, R., and Saake, B. (2006). Size-exclusion chromatography of technical lignins in dimethyl sulfoxide/water and dimethylacetamide. *J. Chromatogr. A* 1102: 154–163.

Salmén, L. (1982). *Temperature and water induced softening behaviour of wood fiber based materials*, Ph.D. thesis, The Royal Institute of Technology, Stockholm.

Salmén, L. and Back, E. (1978). Effect of temperature on stress-strain properties of dry papers. *Sven. Papperstidn.* 81: 341–346.

Sammons, R.J., Harper, D.P., Labbé, N., Bozell, J.J., Elder, T., and Rials, T.G. (2013). Characterization of organosolv lignins using thermal and FT-IR spectroscopic analysis. *BioResources* 8: 2752–2767.

Sapouna, I. and Lawoko, M. (2021). Deciphering lignin heterogeneity in ball milled softwood: unravelling the synergy between the supramolecular cell wall structure and molecular events. *Green Chem.* 23: 3348–3364.

Schwanninger, M. and Hinterstoisser, B. (2002). Klason lignin: modifications to improve the precision of the standardized determination. *Holzforschung* 56: 161–166.

Sevastyanova, O., Helander, M., Chowdhury, S., Lange, H., Wedin, H., Zhang, L., Ek, M., Kadla, J.F., Crestini, C., and Lindström, M.E. (2014). Tailoring the molecular and thermo–mechanical properties of kraft lignin by ultrafiltration. *J. Appl. Polym. Sci.* 131: 40799.

Shrestha, B., le Brech, Y., Ghislain, T., Leclerc, S., Carré, V., Aubriet, F., Hoppe, S., Marchal, P., Pontvianne, S., Brosse, N., et al. (2017). A multitechnique characterization of lignin softening and pyrolysis. *ACS Sustain. Chem. Eng.* 5: 6940–6949.

Souto, F. and Calado, V. (2022). Mystifications and misconceptions of lignin: revisiting understandings. *Green Chem.* 24: 8172–8192.

Startsev, O.V., Makhonkov, A., Erofeev, V., and Gudojnikov, S. (2017). Impact of moisture content on dynamic mechanical properties and transition temperatures of wood. *Wood Mater. Sci. Eng.* 12: 55–62.

Sun, Q., Khunsupat, R., Akato, K., Tao, J., Labbé, N., Gallego, N.C., Bozell, J.J., Rials, T.G., Tuskan, G.A., Tschaplinski, T.J., et al. (2016). A study of poplar organosolv lignin after melt rheology treatment as carbon fiber precursors. *Green Chem.* 18: 5015–5024.

Sun, X.-F., SunFowler, P., and Baird, M.S. (2005). Extraction and characterization of original lignin and hemicelluloses from wheat straw. *J. Agric. Food Chem.* 53: 860–870.

Terashima, N., Kitano, K., Kojima, M., Yoshida, M., Yamamoto, H., and Westermark, U. (2009). Nanostructural assembly of cellulose, hemicellulose, and lignin in the middle layer of secondary wall of ginkgo tracheid. *J. Wood Sci.* 55: 409–416.

Vikström, B. and Nelson, P. (1980). Mechanical properties of chemically treated wood and chemimechanical pulps. *TAPPI J.* 63: 87–91.

Vishtal, A. and Retulainen, E. (2014). Boosting the extensibility potential of fibre networks: a review. *BioResources* 9: 7951–8001.

Vural, D., Gainaru, C., O'Neill, H., Pu, Y., Smith, M.D., Parks, J.M., Pingali, S.V., Mamontov, E., Davison, B.H., Sokolov, A.P., et al. (2018). Impact of hydration and temperature history on the structure and dynamics of lignin. *Green Chem.* 20: 1602–1611.

Wang, C., Kelley, S.S., and Venditti, R.A. (2016). Lignin-based thermoplastic materials. *ChemSusChem* 9: 770–783.

Ward, I.M. and Sweeney, J. (2004). *An introduction to the mechanical properties of solid polymers*. Wiley, Chichester.

Wu, G., Liu, Y., and Shi, G. (2021). New experimental evidence for thermodynamic links to the kinetic fragility of glass-forming polymers. *Macromolecules* 54: 5595–5606.

Wu, S. and Argyropoulos, D. (2003). An improved method for Isolating lignin in high yield and purity. *J. Pulp Pap. Sci.* 29: 235–240.

Yuan, T.-Q., Sun, S.-N., Xu, F., and Sun, R.-C. (2011). Characterization of lignin structures and lignin–carbohydrate complex (LCC) linkages by quantitative 13C and 2D HSQC NMR spectroscopy. *J. Agric. Food Chem.* 59: 10604–10614.

Zhang, L., Larsson, A., Moldin, A., and Edlund, U. (2022). Comparison of lignin distribution, structure, and morphology in wheat straw and wood. *Ind. Crops Prod.* 187: 115432.

Zinovyev, G., Sulaeva, I., Podzimek, S., Rössner, D., Kilpeläinen, I., Sumerskii, I., Rosenau, T., and Potthast, A. (2018). Getting closer to absolute molar masses of technical lignins. *ChemSusChem* 11: 3259–3268.

**Supplementary Material:** This article contains supplementary material (https://doi.org/10.1515/hf-2023-0111).